

TagTrack: Device-Free Localization and Tracking Using Passive RFID Tags

Wenjie Ruan, Lina Yao, Quan Z. Sheng,
Nickolas J.G. Falkner
School of Computer Science
The University of Adelaide
Adelaide, SA 5005, Australia
{wenjie.ruan, lina.yao}@adelaide.edu.au

Xue Li
School of Information Technology
and Electrical Engineering
The University of Queensland
Brisbane, Queensland 4072, Australia
xueli@itee.uq.edu.au

ABSTRACT

Device-free passive localization aims to localize or track targets without requiring them to carry any devices or to be actively involved with the localization process. This technique has received much attention recently in a wide range of applications including elderly people surveillance, intruder detection, and indoor navigation. In this paper, we propose a novel localization and tracking system based on the Received Signal Strength field formed by a set of cost-efficient passive RFID tags. We firstly formulate localization as a classification task, where we compare several state-of-the-art learning-based classification methods including k Nearest Neighbor (k NN), Multivariate Gaussian Mixture Model (GMM) and Support Vector Machine (SVM). To track a moving subject, we propose two Hidden Markov Model (HMM)-based methods, namely GMM-based HMM and k NN-based HMM. k NN-based HMM extends k NN into a probabilistic style to approximate the Emission Probability Matrix in HMM. The proposed methods can be easily applied into other fingerprint-based tracking systems regardless of their hardware platforms. We conduct extensive experiments and the results demonstrate the effectiveness and accuracy of our approaches with up to 98% localization accuracy and an average of 0.7m tracking error.

Categories and Subject Descriptors

C.4 [Special-Purpose and Application-Based System]: Realtime and RFID-based system

Keywords

Localization, RFID, Hidden Markov Model, Gaussian Mixture Model, Kernel-based, Nearest Neighbor

1. INTRODUCTION

Ambient intelligence has been drawing growing attention recently since it enables a smart environment which can

respond to people's locations and behaviors using various wireless signals, sensors, and radio frequency identification (RFID). Under such smart environments, many attractive applications can be realized, which will have huge impact to our daily lives, such as aged care, surveillance, and indoor navigation [17]. A key prerequisite of enabling this intelligence is to localize and track people in the indoor environments. Over the past decade, localization and tracking has been an active research area with several proposed solutions such as LANDMARC [5], WILL [14], and Nuzzer [11].

RFID-based localization has gained much interest due to its low-cost, easy deployment and scalability. Recently, many RFID-based techniques for localization have been proposed [5, 6, 8, 13]. Most of these techniques, however, require the target subject to either carry a tag/reader or be actively involved with the localizing process, which might not be practical. For instance, the attached tag/reader may be lost or damaged, or elderly people with dementia may forget to carry the device. As a result, a device-free RFID-based passive localization solution is highly desirable. Localizing and tracking subjects using such a solution does not require subjects to carry any devices (e.g., wearable sensors or tags).

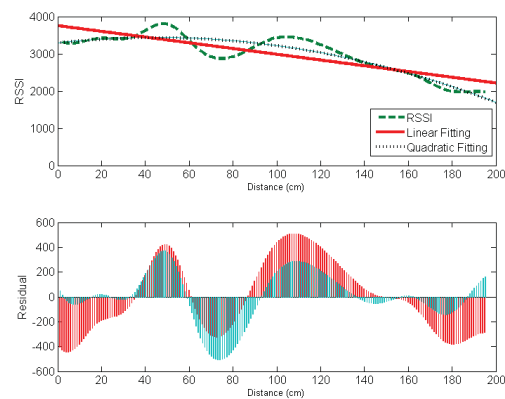


Figure 1: RSSI variation with distance

It is well known that Received Signal Strength (RSS) is quite complicated in real environments due to variability caused by multipath effects and ambient noise interference, physical antenna orientation, and fluctuations in the power source. The signal attenuates while increasing the distance. Figure 1 shows the relationship between Received Signal Strength Indicator (RSSI) of a passive RFID tag and its

Permission to make digital or hard copies of all or part of this work for personal or classroom use is granted without fee provided that copies are not made or distributed for profit or commercial advantage and that copies bear this notice and the full citation on the first page. To copy otherwise, to republish, to post on servers or to redistribute to lists, requires prior specific permission and/or a fee.
MOBIQUITOUS 2014, December 02-05, London, Great Britain
Copyright © 2014 ICST 978-1-63190-039-6
DOI 10.4108/icst.mobiquitous.2014.258004

distance to an antenna. The RSSI does not strictly decrease with the increase of distance, which cannot be expressed by a linear or even a quadratic model. Thus, RSSI is highly nonlinear and uncertain in a complex environment, which may be further corrupted when introducing people's presence or mobility. However, on the other hand, some underlying distinguishable patterns can be observed like how people disturb the pattern of RSS through certain learning-based probabilistic methods. In this work, we deploy passive RFID tags in the corners of the monitored area (see Figure 2) which can form an RSS field (quantified by a 4-dimensional RSSI vector). When a subject appears in different locations inside the monitored area, the RSSI vector will present different patterns. According to aforementioned observations, our proposed approach works on the following two intuitions:

- When a subject presents in an RSS field, the RSSI vector in this field will change compared with the static environment (no subject in this area).
- When a subject appears in different locations in an RSS field, the RSSI vector of this field will embody different fluctuation patterns.

Device-free RFID-based passive localization in general works as follows. The RSSI vectors are first collected when people present in various predefined locations, and then a given testing location is mapped to one of these trained locations based on the observed RSSI vector. Two existing research efforts on RFID-based device-free localization [4, 20] are based on the first intuition, which explore people's location based on an array of densely-deployed active tags [4] or an array of mixed passive and active tags [20]. In this paper, we propose a new approach by considering both intuitions. Our approach not only captures the binary information of RSSI, but also quantifies the variation information to decode a more accurate location. We verify our approach by setting up a testbed. In particular, we deploy passive RFID tags and an RFID antenna as a single RSS field (as showed in Figure 2). A sequence of RSSI vectors collected from various known locations along with corresponding correct location labels are used to train a model, which is then used to estimate the subject's location for a given new RSS vector. Our main contributions are summarized as follows:

- We introduce a pure passive tag-based localization and tracking system and our experimental studies demonstrate the feasibility and accuracy of the proposed approach. To the best of our knowledge, our work is one of first few to deal with device-free passive localization and tracking based on pure passive RFID tags.
- We propose k NN-based HMM and GMM-based HMM methods, which track a moving subject by learning underlying patterns of a stationary subject in different locations. Specially, we transfer traditional k NN classifier into a probabilistic style to estimate the emission matrix in HMM, which bridges the gap between tracking and localization.
- We demonstrate the scalability of our system by expanding a single RSS field into multiple RSS fields. More importantly, our method can achieve an accuracy over 94% while reducing the training overhead (collecting only 12 seconds training samples per grid), which significantly simplifies the calibration stage.

The rest of the paper is organized as follows. Section 2 overviews related work on localization and tracking. We present our environment setting and initial experiments for intuition verification in Section 3 and formulate our research problems in Section 4. Section 5 presents our proposed solutions, and the experimental results and analysis are presented in Section 6. Finally, Section 7 offers some concluding remarks.

2. RELATED WORK

Localization has been an active research area over the decades. In this section, we first review some state-of-the-art localization systems, and then focus on RFID-based device-free passive localization which is more related to our work.

Criquet [7] adopts an ultrasonic Time-Of-Flight (TOF)-based method to locate target subjects which carries a Bat (transmitter) periodically emitting a short pulse of ultrasound. In [5], Ni et al. design a system to localize the target object carrying an active RFID tag. It employs densely deployed RFID tags to alleviate the fluctuation feature in RSSI and then estimates target location by matching the measurements with the stored fingerprints. With the popularity of smart phones, FTrack [18] proposes to use the accelerometer in mobile phones to capture user encounters and trails for locating the number of floor levels where people present. WILL [14] presents a wireless indoor localization approach to locate people's positions, requiring no prior knowledge of access point locations. All these systems require a tracked entity to carry a device (e.g., RFID reader/tags or mobile phones), which might be impractical for some applications.

Device-free localization recently has become an active research area since Youssef et al. first identify the challenges of device-free passive localization in [19]. Most recent state-of-the-art localization and tracking systems are based on wireless sensor networks. Patwari et al. [21] propose a kernel distance-based RTI (radio tomographic imaging) by using a kernel distance of histograms to locate a moving or stationary person based on wireless TelosB nodes. Nuzzer [11] estimates the location of entities by monitoring the RSS at certain monitoring points using wireless networks, which first constructs a passive radio map in an offline style, and then uses a Bayesian-typed inference algorithm to optimize a location with the largest probability. Xu et al. [16] develop a fingerprinting-based device-free passive localization system, in which several discriminant analysis approaches are explored. In [15], the authors further extend the system to count and localize multiple subjects based on the same hardware platform, in which they first iteratively estimate the number of subjects by a successive cancellation algorithm and then a conditional random field (CRF) is used to localize multiple subjects simultaneously. Ichnaea introduced by [9] realizes the device-free passive motion tracking by exploring several statistical anomaly detection methods, an anomaly scores-based particle filter model, and a human motion model.

WSNs-based localization systems require maintenance (e.g., replacing batteries). In contrast, passive RFID-based localization systems are cost-efficient (cheap passive tags), easy to deploy, and maintenance-free. Recently, some research efforts have been proposed to deal with the device-free passive localization based on RFID technology. For instance, based on densely-deployed passive tags, [12] utilizes RTI for device-free indoor localization. Twins [3] is another very re-

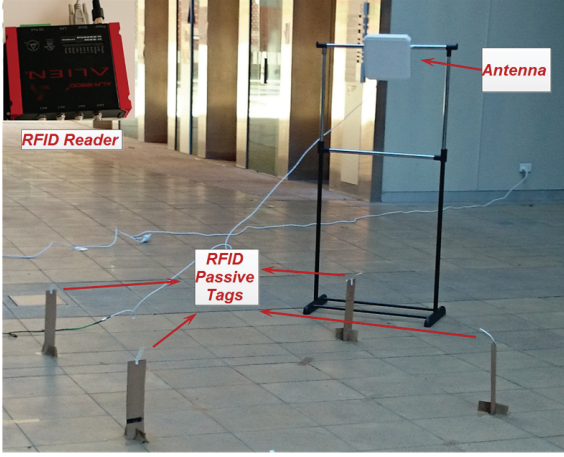


Figure 2: Hardware Setup

cent system, which leverages observations caused by interference among passive tags to detect a single moving subject. Liu et al. [4] propose to deploy active tags into an array, which captures localization information when the RSSIs of tags (known position) variate beyond a threshold, and frequent trajectory patterns can be mined based on estimated localization sequences. Zhang et al. [20] develop another tag array-based localization scheme using both active and passive tags, which is more cost-efficient and much effective on RSSIs noise reduction. However, those two schemes focus more on mining frequent trajectory patterns and only model the mapping from the binary information of tags (RSSIs changed bigger than a threshold or not) to locations rather than quantifying variation of RSSIs to locations. By comparison, our approach explores the relations between variation of RSSIs and locations, and only based on “pure” passive RFID tags, which are more cost-efficient and practical (e.g., no maintenance needs).

3. SYSTEM OVERVIEW

In this section, we introduce our system hardware setup and conduct several preliminary experiments to verify our assumptions (two intuitions mentioned in the introduction).

3.1 Hardware Deployment

Figure 2 shows hardware, including an Alien ALR-9900+ Enterprise RFID Reader ($20.3cm \times 17.8cm \times 4.1cm$), two circular antennas ($20cm \times 20cm \times 3cm$), and squiggle Higgs-4 passive tags ($1cm \times 10cm$). The reader operates at 840-960MHz and supports UHF RFID standards such as ETSI EN 302 208-1. We set the sample rate as 0.5s and each tag reading contains a timestamp, a tag ID and an RSSI value, which are processed by a computer with an I7-3537U 2.5GHz processor and 8G RAM, running in WINDOWS 7.

We describe our antenna and tag placement strategies show an RSS field formed by passive tags (see Figure 2), which can be easily extended into a larger area by combining multiple RSS fields (see Figure 7).

Antenna Placement: Ideally, all tag readings should be captured by the antenna. Based on our preliminary experiments, we place the antenna in 1.5m above the ground, facing tags with approximately 45° . However, during the localization and tracking, an antenna can not guarantee to read

all tags, particularly for passive tags. We solve the problem based on a fingerprint framework and develop a strategy to deal with missing readings.

Tags Placement: Tags can be deployed in any geometric shape since our proposed approach targets to learn a model mapping different RSS distribution patterns to its corresponding locations. For the simplicity, we place tags as a square-shaped array.

Reading RFID tags: To be consistent and easy to feed into algorithms, we send an RSSI request to all tags within a sampling time. If we cannot receive RSSI readings of a certain tag, the RSSI value is set to 0. Thus, mathematically, for all the time stamps, we have the RSSI vectors with the same dimensions. In our settings, the tag detection range can be up to 6 meters.

3.2 Intuitions Verification

In this section, we verify the two intuitions discussed in Section 1. First, we design a simple testbed (see Figure 2) which is a standard single RSS field formed by 4 passive tags (in 4 corners) and an antenna. Then, we manually divide the field into 9 virtual grids, which represent 9 different locations l_1, l_2, \dots, l_9 . To verify the intuitions, we compare the patterns of RSSI vector when a subject is located in different locations.

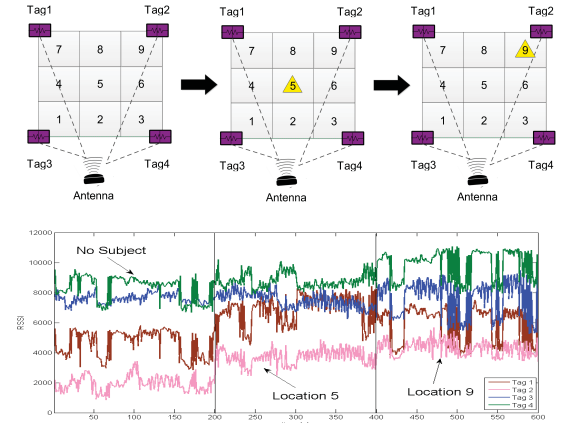


Figure 3: RSSI vector are different due to the presence of the subject in different locations

Figure 3 depicts different RSSI patterns when a subject presents in different locations. When the subject appears in different locations, the RSSI vector shows different fluctuation patterns, which confirms our intuitions. Therefore, our preliminary studies have shown the feasibility and potential of RSS field formed by sparse deployment of passive tags for solving localization and tracking problems.

4. PROBLEM FORMULATION

In this paper, we target the following two main problems, which are the key issues to realize device-free passive localization and tracking.

PROBLEM 1 (LOCALIZATION). *Can we reliably localize the monitored subject by learning the RSSI changes? Namely, given a sequence of RSSI vectors, reliably localizing a stationary subject.*

PROBLEM 2 (TRACKING). *Can we accurately track the moving subject by learning the RSSI changes? Namely, given a continuous sequence of RSSI vectors, accurately estimate the trajectory of a moving subject.*

The location estimation in this paper is regarded as a classification problem where the task is to model how the signal strengths are distributed in different geographical areas based on a sample of measurements collected at several known locations.

We divide our testing area formed by D anchoring passive tags into J grids, denoted by $\mathbf{l} = (l_1, \dots, l_J)$, $\mathbf{S} = [\mathbf{s}_1, \dots, \mathbf{s}_N]^T$, where $\mathbf{s} \in \mathbb{R}^D$, D is the number of anchoring passive tags. We first measure the RSSI values for all anchoring tags when the testing area is empty. Then a single subject appears in J predefined grid and takes another collection of RSSI values. As a result, we obtain profiling data \mathcal{H} , which is a $(J+1) \times N \times D$ matrix, quantifies how a subject affects the RSSI from each grid plus the environmental RSSI without a subject. Then, we can use \mathcal{H} to train the model and get the model parameters. By the end of the training phase, we build a $(J+1)$ -class classifier.

In the testing phase, we collect the continuous new RSSI vectors when a subject shows up or walks in random grids, and the RSSI vectors forming observation data $\mathcal{O} = \{\mathbf{o}_1, \mathbf{o}_2, \dots, \mathbf{o}_T\}$ implies how this subject's presence or moving impact the RSSI from random unknown grids. Then, we put \mathcal{O} into the $(J+1)$ -class classifier obtained in the training phase to assign the subject a grid number. Problem 1 can be formulated as finding the optimal posterior distribution $p(l_j|\mathbf{o}_i)$ given a new sequence of observed RSSI vectors.

$$j^* = \arg \max_j Pr(l_j|\mathbf{o}_i) \quad (1)$$

Problem 2 can be formulated as tracking a moving subject described by its state as location l_t at time t , with dynamic motion specified by $Pr(l_t|l_{t-1})$ given a continuous sequence of RSSI vectors. In order to do this, we can maintain a distribution over a sequence of observable RSSI $\mathcal{O}_{1:T}$ and corresponding locations $l_{1:T}$:

$$Pr(\mathbf{o}_{1:T}, l_{1:T}) = Pr(l_1)Pr(\mathbf{o}_1|l_1) \prod_{t=2}^T Pr(\mathbf{o}_t|l_t)Pr(l_t|l_{t-1}) \quad (2)$$

to estimate the expected l_t under this distribution. A moving subject is described by its location l_j , with motion specified by a Markovian dynamic model $Pr(l_j|l_{j-1})$. We need to have a marginal posterior $Pr(\mathbf{s}_i|l_{1:j})$ and estimate the expected value of l_j under this distribution.

In the rest of this paper, we will introduce technical details on how these two problems are solved.

5. PROPOSED SOLUTIONS

5.1 Localizing Stationary Subjects

For the localization problem, we introduce three state-of-the-art learning-based classification methods, namely the *Multivariate Gaussian Mixture Model*, the *k Nearest Neighbor*, and the *Support Vector Machine*.

5.1.1 Gaussian Mixture Model

As stated in Equation 1, our goal is to maximize $Pr(l_j|\mathbf{o}_i)$. It should be noted that we will drop the subscript i and j for the sake of simplicity and clarity in descriptions.

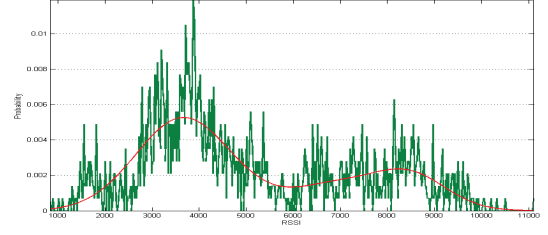


Figure 4: Distribution pattern of RSSI and fitted by learned GMM with two components

$$\begin{aligned} \arg \max_{l \in \mathcal{L}} Pr(l|\mathbf{o}) &= \arg \max_{l \in \mathcal{L}} \frac{Pr(\mathbf{o}|l)Pr(l)}{Pr(\mathbf{o})} \\ &\propto \arg \max_{l \in \mathcal{L}} Pr(\mathbf{o}|l) \cdot Pr(l) \end{aligned} \quad (3)$$

where $Pr(l)$ is the probability of finding the subject at location l , which is set as a uniform distribution $Pr(l) \sim \frac{1}{J}$. We adopt the well-known idea of mixture models in statistics. We first make a general assumption that the subject could be in any of J grids with varying probabilities. Each of these probabilities potentially generate a distribution of RSSI vectors at each grid.

The key is to find the appropriate model that describes $Pr(\mathbf{s}|l)$ distribution. We assume this distribution of each grid l follows a Gaussian Mixture Model with q_m^l components, mean $\mu_{l,m}^l$ and covariance matrix $\Sigma_{l,m}^l$:

$$\begin{aligned} f_l(x) &= Pr(x|l) = \sum_{m=1}^M q_{l,m} \mathcal{N}(x|\mu_{l,m}, \Sigma_{l,m}) \\ &= \sum_{m=1}^M \frac{q_{l,m}}{\sqrt{(2\pi)^D |\Sigma_{l,m}|}} \exp\left(-\frac{1}{2}(x - \mu_{l,m})^T \Sigma_{l,m}^{-1} (x - \mu_{l,m})\right) \end{aligned} \quad (4)$$

where $\Phi_l = \{q_{l,m}, \mu_{l,m}, \Sigma_{l,m}\}$ is the model parameter set at grid l , q_m is the mixture weighted factor that describes the prior probability of the m^{th} mixture component, and the $\mu_{l,m}$ and $\Sigma_{l,m}$ are the mean and covariance of the m^{th} Gaussian distribution. For each grid, the maximum likelihood estimation $\hat{\Phi}_l$ of Φ_l can be expressed as:

$$\hat{\Phi}_l = \arg \max_{\Phi_l} Pr(x|l, \Phi_l) = \arg \max_{\Phi_l} \prod_{i=1}^N Pr(\mathbf{s}_i|l, \Phi_l) \quad (5)$$

where $\mathbf{s} = \{\mathbf{s}_1, \mathbf{s}_2, \dots, \mathbf{s}_N\}$ is the training set.

We use the Expectation Maximization (EM) to solve Equation 5. The EM algorithm is an iterative process consisting of two steps: the *expectation* step (E-step) and the *maximization* step (M-step). The E-step is to find the posterior probability $Pr(l|\mathbf{s})$ given training RSSI set \mathbf{s} . The M-step is to maximize the expected log-likelihood of the observed data. This leads us to re-estimate the parameters for the next iteration based on the posterior probabilities calculated. During the iterations, we generate a sequence of model parameters $\Phi_l^0, \Phi_l^1, \dots, \Phi_l^*$, where Φ_l^0 is the initial parameter and Φ_l^* is the converged parameter when the algorithm terminates with satisfying predefined conditions. We adopt the Akaike Information Criterion (AIC) [1] as the

criterion to select the best number of components for each GMM. Figure 4 shows the fitted GMM of RSSI with two components.

After learning the model parameters with EM, given the new RSSI signals \mathbf{o} collected from the array of tags, the probability that the subject may present at certain grids is calculated according to the GMM parameters Φ_l on each grid. The location with maximal probability is taken as the predicted location of the subject.

5.1.2 k Nearest Neighbor

Nearest neighbour is based on some context dependent distance measure that assigns an Euclidean distance between any two RSSI samples. Given a set of training RSS data and a testing RSS vector, the location is estimated from the training samples whose observation RSS vector has the minimal distance when compared with the testing observation. In particular, a testing RSSI sample is classified by a majority vote of its neighbors, with the RSSI being assigned to the grid most common among its k Nearest Neighbors. In the case of tied votes, we choose the nearest neighbor among the k nearest neighbors.

5.1.3 Kernel-based Localization

Kernel-based learning (KL) methods localize objects based on the fact that the smaller the distance between two RSSI samples, the higher probability they are in the same or a close location. Specifically, a sequence of RSSI is used as the training set for a learning procedure. The result of this procedure is a prediction model that will be used to localize subject to previously unknown positions. A probability mass is assigned to a kernel around each of observable RSSI in the training data. Thus the resulting density estimate for an observation \mathbf{o} in location l is a mixture of n_1 equally weighted density functions, where n_1 is the number of training data l :

$$k_{rbf}(\mathbf{o}_i; \mathbf{o}_j) = \frac{1}{\sqrt{2\pi}\sigma} \exp\left(-\frac{(\mathbf{o}_i - \mathbf{o}_j)^2}{2\sigma^2}\right) \quad (6)$$

We compare the RBF kernel, linear kernel and polynomial kernel in this paper to model pairwise similarity of RSSI vectors in the feature space.

$$k(\mathbf{o}_i, \mathbf{o}_j) = (||\mathbf{o}_i - \mathbf{o}_j|| + c)^d \quad (7)$$

where c and d are parameters to be determined in real applications.

We use LibSVM [2] to implement the kernel-based localization. The choice of kernels is highly dependent on the nonlinear and noisy characteristics of the localization problem due to possible path loss, shadowing and multipath effects etc. We examine the linear kernel, Gaussian kernel and polynomial kernel, and find that the SVM classifier performs the best with linear kernel in this work.

5.2 Tracking Moving Subjects

To track a moving subject, we propose two Hidden Markov Model-based methods, namely GMM-based HMM and k NN-based HMM, to decode the sequential RSSI observations into continuous subject's trajectories. HMM has shown tremendous success in spatio-temporal features recognition, and its basis elements are briefly described as the following. Given \mathbf{O} is the observed sequence of RSSI vectors and \mathbf{L} denotes the location sequence of the monitored subject, our goal is

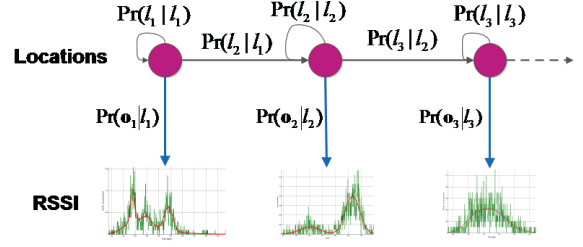


Figure 5: GMM-based HMM

to find the most likely location sequences \mathbf{L}^* , which can be denoted as:

$$\mathbf{L}^* = \arg \max_{\mathbf{L}} Pr(\mathbf{L}|\mathbf{O}) \quad (8)$$

Specifically, we define a distribution over a sequence of observable RSSI $\mathbf{O}_{1:T}$ and the corresponding locations $l_{1:T}$:

$$Pr(\mathbf{o}_{1:T}, l_{1:T}) = Pr(l_1) Pr(\mathbf{o}_1 | l_1) \prod_{t=2}^T \underbrace{Pr(\mathbf{o}_t | l_t)}_B \underbrace{Pr(l_t | l_{t-1})}_A \quad (9)$$

Thus, the HMM recognition approach can be divided into three main steps, namely *emission matrix*, *state matrix*, and *viterbi searching*:

- Emission Matrix B : Given RSSI sequence $\mathbf{O} = \{\mathbf{o}_1, \dots, \mathbf{o}_i\}$, calculating the probability of each RSSI \mathbf{o}_i belonging to each grid l_j , denoted as $Pr(\mathbf{o}_i | l_j)$.
- Transition Matrix A : Calculating the probability of a subject moving from grid l_i to grid l_j . The probability is denoted as: $Pr(l_j | l_i)$.
- Viterbi Searching: Searching the most likely sequence of grids $\{l_1, l_2, \dots, l_j\}$, given a continuous sequence of observation RSSI vectors $\{\mathbf{o}_1, \mathbf{o}_2, \dots, \mathbf{o}_j\}$.

5.2.1 Emission Matrix

The emission matrix $B_{ij} = Pr(\mathbf{o}_i | l_j)$ in our case infers the current state based on the observation RSSI vector \mathbf{o} at each time stamp, which generates a grid likelihood map in terms of corresponding \mathbf{o} . We aim at maximizing the likelihood $Pr(l_j | \mathbf{o}_i)$ when grid i is occupied. In other words, we would like to maximize the probability that the estimated grid i matches the actually occupied grid.

GMM-based HMM. For GMM-based HMM (see Figure 5), we propose to use GMM to produce its Emission Matrix that can be obtained from Equation 4 in Section 5.1.1. As for the static subject case, we assume the observed RSSI vectors in each location follow a multivariate Gaussian mixture model (Equation 4 defined in Section 5.1.1):

$$Pr(\mathbf{o}_i | l_j) = \sum_m^M q_m N(\mu_m, \Sigma_m) \quad (10)$$

kNN-based HMM. In Section 5.1.2, we use k NN to classify unknown RSS vectors, which obtain the best accuracy among other popular classification methods. Thus, for the tracking problem, we extend the traditional k NN into a probabilistic style, in which, for each possible state, the proposed k NN method will give an emission probability based

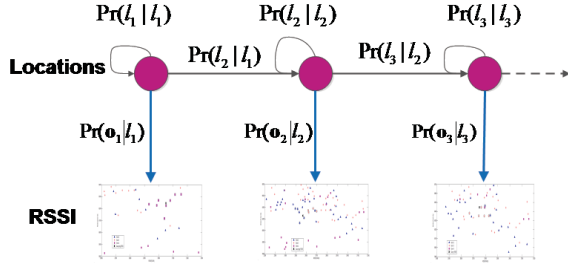


Figure 6: k NN-based HMM

on current observed RSSI vector (see Figure 6). To the best of our knowledge, we are the first to introduce the k NN-based HMM for the tracking problem, which can be generally applied into other fingerprint-based tracking systems. Specifically, k NN-based HMM approach would be obtained as: assuming for each observation \mathbf{o}_j , we search its k Nearest Neighbors from the training set \mathbf{s} , denoted as $N(\mathbf{o}_j)$, and $N^i(\mathbf{o}_j) = \{\mathbf{s}_k | \mathbf{s}_k \in N(\mathbf{o}_j) \cap \mathbf{s}_k \in l_i\}$, and emission matrix is:

$$Pr(\mathbf{o}_j | l_i) = \frac{\sum_{\mathbf{s}_k \in N^i(\mathbf{o}_j)} \frac{1}{dis(\mathbf{o}_j, \mathbf{s}_k)}}{\sum_{\mathbf{s}_{k'} \in N(\mathbf{o}_j)} \frac{1}{dis(\mathbf{o}_j, \mathbf{s}_{k'})}} \quad (11)$$

where $dis(\mathbf{o}, \mathbf{s})$ indicates the Euclidean distance between two RSSI vectors \mathbf{o} and \mathbf{s} .

5.2.2 Transition Matrix

Transition matrix measures the probability of a subject commutes to next location at time t . The transition is a Markov process where each state is conditionally independent of all other states given the previous state, which can be defined as $A_{ij} = Pr(a_t = l_i | a_{t-1} = l_j)$. However, from commonsense, a subject can only move a step at a time, meaning that it is highly unlikely for the subject to move from the lower-left corner to the upper-right corner (e.g. in Figure 9, from location 53 to location 22). Therefore, we adopt two transition strategies to calculate the next state for each given current state, defined as follows:

- Transition without Constraint. The monitored subject can move to any locations in this testing area without any transition constraint under equal probabilities.
- Transition with Constraint. The monitored subject can only move to a location which is *adjacent* (including current location which means still) to current location with equal probabilities. The probabilities of moving to other locations are *zero*.

Since we do not know when people will change their moving directions, we assume that, to simplify our model, people move to other legitimate locations with equal probabilities. Based on the two strategies, we propose two types of transition matrix in HMM. We can model our two different transition processes as one. Assuming we have J locations: $J = \{l_1, l_2, \dots, l_i, \dots, l_J\}$, each location l_i denotes the subject appears in grid i . Assuming for current state l_i , all the possible states the subject can move to belong to the set Ω_i , and the number of states contained in the set is $|\Omega_i|$. Thus

the transition probability matrix can be expressed as:

$$Pr(l_j | l_i) = \begin{cases} \frac{1}{|\Omega_i|} & \text{if } l_j \in \Omega_i \\ 0 & \text{if } l_j \notin \Omega_i \end{cases} \quad (12)$$

5.2.3 Viterbi Searching

The Viterbi algorithm defines $V_j(t)$, the highest probability of a single path of length t which accounts for the first t observations and ends in state l_j :

$$V_j(t) = \arg \max_{l_1, l_2, \dots, l_{t-1}} Pr(l_1 l_2 \dots l_t = j, \mathbf{o}_1 \mathbf{o}_2 \dots, \mathbf{o}_t | A, B) \quad (13)$$

where A and B can be found in Equation 9. Further, we can have:

$$\begin{aligned} V_j(1) &= B_j(\mathbf{o}_1) \\ V_j(t+1) &= \arg \max_i V_i(t) A_{ij} B_j(\mathbf{o}_{t+1}) \end{aligned} \quad (14)$$

where $B_j(\mathbf{o}_1) = Pr(\mathbf{o}_1 | l_j)$ and $A_{ij} = Pr(l_j | l_i)$. Finally, we can estimate the optimal path with maximum likelihood for GMM-based HMM and k NN-based HMM, sketched by Figure 5 and Figure 6.

5.2.4 Forward Calibration

When applying the proposed approach to tracking, we find some latency in detecting a subject in the corresponding grid, which is mainly caused during the RSSI collection process and by the delay of signals sent by passive tags [10]. The RSSI collector is programmed with a timer to poll the RSSI with a predefined order of transmission, taking around 1 second to complete a new measurement with no workarounds. To cope with the impact of this latency, we adopt a forward calibration mechanism to calibrate the estimated location sequences to offset the latency, which uses a moving time averaging window to recalculate the coordinates of location sequence obtained by Viterbi Searching. Specifically, the technique estimates the location coordinates by averaging the last few location coordinates obtained by either the discrete space estimator or the spatial averaging estimator. The estimated location l_t at time t can be calculated using:

$$\hat{c}'_t = \frac{\sum_{i=t}^{t+|w|-1} \hat{c}_i}{|w|} \quad (15)$$

where $|w|$ is the window length. \hat{c}_i is uncalibrated coordinates of the center of predicted grids at time t by Equation 13.

6. EXPERIMENTS

We first tested our methods in a standard RSS field (Figure 2), in which we virtually divided a testing area into 9 grids, with each grid of $0.6m \times 0.6m$ in size. Then we conducted a multi-RSS field experiment (Figure 7) to test the robustness and scalability of our approaches, in which we combined 6 RSS fields to monitor a $3.2m \times 4.8m$ testing area and divided each RSS field into 4 virtual grids.

6.1 Data Collection and Metrics

The RFID reader monitored and collected RSSI values at the sampling rate of 0.5s. We collected training RSSI measurement from tags for each grid based on two strategies [16]. In the first case, the subject stood at the center of each grid and span around so that the resulting training data would



Figure 7: Multiple RSS fields Experiment

focus on the grid center but involve different orientations. In the second case, the subject walked randomly within the cell. For each case, we collected training data for one minute in each virtual grid. Thus we spent 20 minutes for the single RSS field experiment and 50 minutes for the multi-RSS field experiment.

We used two metrics, *accuracy* and *error distance*, to measure our proposed approaches in terms of localization and tracking respectively. The accuracy is defined by:

$$Acc. = \frac{\sum_i^N \mathbb{I}(\hat{l}_i, l_i)}{N} \quad (16)$$

where $\mathbb{I}(a, b)$ is an indicator, which is 1 if a is equal to b , 0 otherwise, \hat{l}_i is the predicted grid, (i.e., the center of the estimated grid), l_i is the actual number of grids, and N is the total number of observation RSSI vectors.

The error distance denotes the averaging accumulated error distance for each grid in each continuous trajectory, defined as

$$Dis_{err.} = \frac{\sum_i^{|T|} dis(\hat{c}_i, c_i)}{|T|} \quad (17)$$

where c_i is the coordinates of the actual coordinates in sampling time i , $dis(\hat{c}_i, c_i)$ is the Euclidean distance between predicted coordinates and actual coordinates, $|T|$ is the total number of test sample generated by a subject in a trajectory.

6.2 Single RSS Field Experiment

Before evaluating our approach in localization and tracking, we need to take care of two main issues: one is about experimental setting, e.g., what is the optimal grid size, and the other is about how to deal with delay issue we found during the experiments. Based on our empirical study during this work, the smaller the grid size, the worse localization accuracy will be due to more indistinguishable disturbance, and more profiling data are needed as well. In our work, high resolution for locations is not our main concern. For instance, in an elderly people assistant system, caregivers are generally interested to know which sub-area or room the elderly is other than a very fine-grained location point. Therefore, in our experiment, we divided one single RSS field into 9 virtual grids, which can locate people in a $0.6m \times 0.6m$ resolution. For the latency, we adopted the forward calibration algorithm to recalculate the coordinates for tracking.

Localization: Figure 8 shows the results of localizing a sub-

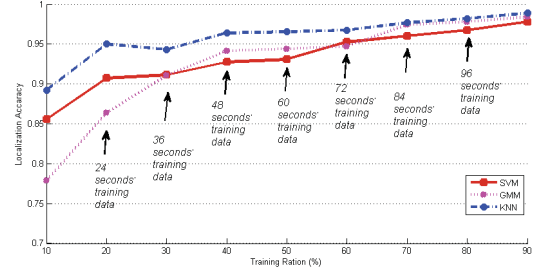


Figure 8: Results Comparison on Localizing a Subject with Different Training Ratio

Table 1: Error distance on tracking a moving subject (m), TC: Transition Constraint

Methods	Without TC	With TC
kNN-based HMM	0.63	0.53
kNN-based HMM + Forward Calibration	0.42	0.35
GMM-based HMM	0.61	0.60
GMM-based HMM + Forward Calibration	0.48	0.39

ject with three different methods on varying training ratios (from 10% to 90%). We used 2 minutes of the mixed data (contained the stationary data and the dynamic data) for training. The test set was collected when target stood in 9 different locations and no presence for 30 seconds each. For the localization experiment in the single RSS field, we set k as 2, which gives the best performance for kNN . The linear kernel is the best setting for SVM. We adopt AIC [1] for selecting the best number of components for each GMM, which mainly range from 2 to 6. Our proposed approach performs very well, and the localization accuracy can reach as high as 98.91% when using all the training data. More importantly, only with 36 seconds training data for each grid, our system can achieve localization accuracy over 90%. Specially, by kNN , we only need to collect 24 seconds training data to get an accuracy as high as 95%. In previous work, the shortest time needed for collecting training data to get same localization accuracy is about 1 minute [16]. Among all the three classifying methods, kNN achieves the best accuracy, which underpins our proposed kNN -based HMM method for detecting motions of a subject.

Tracking: Table 1 shows the results on tracking a moving subject using GMM-based HMM and kNN -based HMM under transition constraint and without transition constraint respectively. We set up one moving path along the grids (see Figure 3): $1 \rightarrow 4 \rightarrow 7 \rightarrow 8 \rightarrow 9 \rightarrow 6 \rightarrow 3 \rightarrow 2 \rightarrow 1$. As the table shows, the kNN -based HMM with forward calibration achieves the best performance, and the tracking error is about 0.35m. It is noted that, for GMM-based HMM, the tracking errors are similar regardless of transition constraints. The reason is that we still use the fixed length moving window to smooth all the raw estimated coordinates in the dynamic tracking case. However, the latencies for different paths and walking velocities are different. In our future work, we will explore a dynamic moving averaging window for an adaptive varying length smoothing.

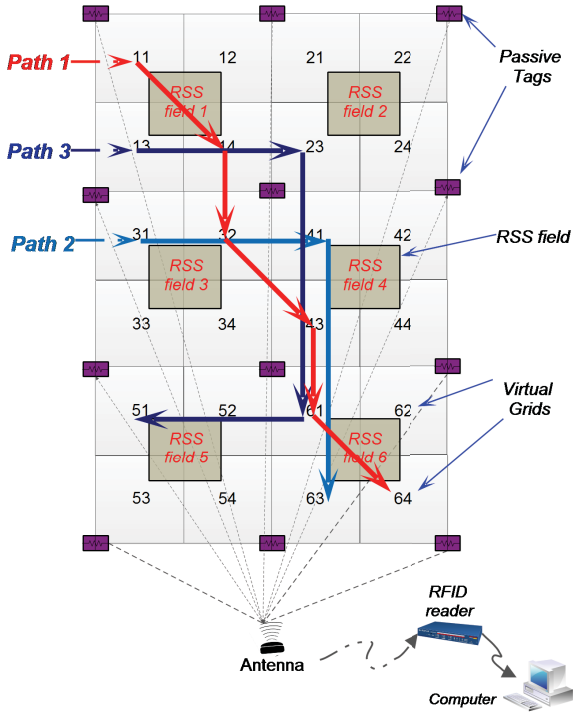


Figure 9: Multiple RSS fields and testing paths

6.3 Multiple RSS Fields Experiment

In this section, we report the experimental results using a larger monitored area stacked by 6 RSS fields.

6.3.1 Results on Localization

To be more practical, we define the following three scenarios in our multiple RSS fields experiment.

SCENARIO 1 (STATIONARY). Assuming a subject stands in an unknown place in the monitored area still, such as watching TV or waiting for someone.

SCENARIO 2 (DYNAMIC). Assuming a subject keeps moving around or performing some activities in a small unknown area, such as cooking in the kitchen or doing exercises in a gym.

SCENARIO 3 (MIXED). Assuming a subject presents in an unknown place who performs a combination of Scenario 1 and Scenario 2, such as doing some exercises for a while and then watching TV.

Based on the predefined three scenarios, we collected three types of data for testing: i) a subject is standing in each grid for 20 seconds, ii) a subject keeps moving around within each grid for 20 seconds, and iii) combining both activities for 40 seconds in each grid. Before that, we also collected one-minute stationary data, 1-minute dynamic data and 2-minute mixed data for each grid, for training purpose. The localization results varying with training ratio (only use partial collected data to train classifiers) are shown in Table 2.

For Scenario 1, all classification methods achieve good accuracy. In particular, we can achieve 94% localization accuracy with only 12 seconds training data per grid by using

Table 2: Localization accuracy on multiple RSS fields. k NN: $k=2$; GMM: component number=4; SVM: linear kernel, termination criterion=0.01, $C=1$, other parameters as default [2].

Scenario	Train. Ratio (%)	20	40	60	80	100
Scenario 1	kNN	0.94	0.94	0.95	0.96	0.98
	GMM	0.88	0.91	0.93	0.96	0.97
	SVM	0.94	0.95	0.95	0.97	0.98
Scenario 2	kNN	0.52	0.58	0.62	0.64	0.66
	GMM	0.48	0.55	0.61	0.62	0.64
	SVM	0.51	0.56	0.56	0.56	0.60
Scenario 3	kNN	0.66	0.67	0.75	0.80	0.81
	GMM	0.60	0.62	0.72	0.79	0.79
	SVM	0.66	0.67	0.74	0.76	0.76

Table 3: Average tracking error on multiple RSS fields (m), TC: Transition Constraint

Methods	Path	Without TC	With TC
kNN-based HMM	Path 1	0.94	0.88
	Path 2	0.89	0.80
	Path 3	0.99	0.93
kNN-based HMM+ Forward Calibration	Path 1	0.94	0.68
	Path 2	0.64	0.65
	Path 3	0.80	0.74
GMM-based HMM	Path 1	1.24	1.42
	Path 2	0.91	0.94
	Path 3	0.84	1.19
GMM-based HMM+ Forward Calibration	Path 1	0.85	1.08
	Path 2	0.71	0.70
	Path 3	0.79	0.57

k NN, which exhibits great advantages than other fingerprint-based schemes. For Scenario 2, the best localization accuracy is 66% achieved by k NN. It is worth to mention that, performance is more sensitive to the size of training data in this case. More training data can better interpret more informative RSSI patterns in this dynamic scenario compared with the stationary scenario. For Scenario 3, the localization accuracy can reach 81%. To conclude, k NN achieves the best localization accuracy and is also more robust to the RSSI uncertainties, especially when the training data is small. It should be noted that GMM and SVM can also achieve reasonably good performance.

6.3.2 Results on Tracking

In this section, we report experimental results on tracking problem. We evaluated the k NN-based HMM and GMM-based HMM on three different paths (Figure 9). In addition, we extensively investigated how to select parameters of the models and how to cope with system latencies.

Table 3 shows our overall tracking performance regarding the three paths, among which k NN-based HMM with forward calibration under the Transition Constraint achieves a better result (average tracking error is 0.7m). However, for Path 3 which is more complicated compared with other two paths, GMM-based HMM with transition constraint has the smallest estimated error of 0.57m. This may lie in fact that GMM can better capture and quantify the mapping from RSSI vector to the likelihood of each possible grid for some complicated trajectories.

Window Size in Forward Calibration: Latency is the most common concern in indoor localization systems [10]. Based on our proposed forward calibration algorithm, one of key issues is to decide the window size. Figure 10 shows the

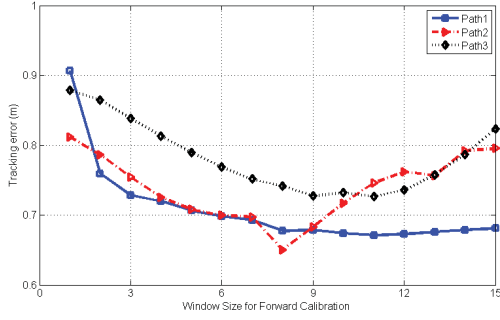


Figure 10: Estimated tracking errors for different window sizes using k NN-based HMM

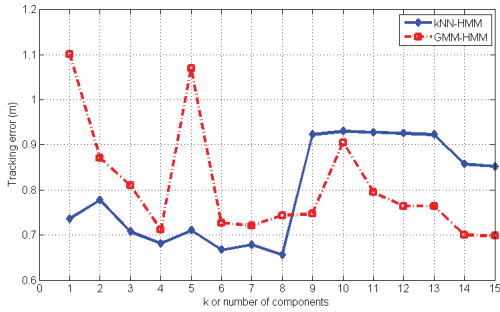


Figure 11: Estimated tracking errors for different k values in k NN-based HMM and component numbers in GMM-based HMM

relevance between the tracking error and the window size of forward calibration when dealing with latency in different paths. We can find that the least tracking error is achieved by window sizes ranged from 8 to 11. To reduce the burden of computational resource, we selected 8 as the optimal window size of forward calibration to reduce the latency.

Parameters Selection: We investigated the parameters setting by using path 2 as an example. As Figure 11 shows, the tracking error slightly decreases and reaches the minimal error when k is 8, which is the best k value for path 2. The red line with square marks exhibits the relation of number of GMM components between tracking error in GMM-based HMM method. For GMM case, the best tracking accuracy can be achieved at 4, 6 or 8 GMM components. However, larger number of components potentially results in problems of overfitting or ill condition especially for the case of small number of training data. Larger number of components also increases the computational cost. We set the number of components as 4 in our experiment.

Stationary Data vs Dynamic Data: We added dynamic training data (before black dot line, the first 50%) as the first stage, and then stationary training data (after black dot line, the last 50%) as the second stage in Figure 12. From the results of k NN-based HMM, estimate error decreases with more training data. More training data can provide more useful anchor RSSI vectors on unknown RSSI vector to make a better majority vote compared with GMM-based HMM. In addition, we observed that the last 40 percent stationary training data do not lead to a better result. However, when

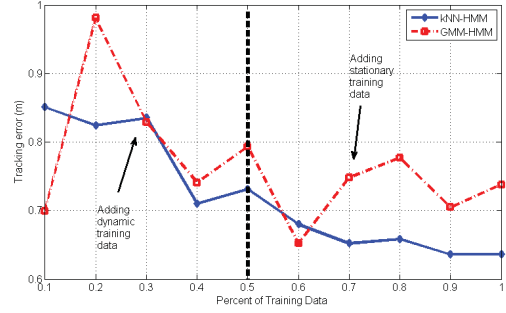


Figure 12: Estimated tracking errors for different percent of training data

adding more dynamic data in the first stage, the estimate error declines from 0.85m to about 0.7m, which indicates the possibility of enhancing the model accuracy by integrating more dynamic data into the training set.

6.4 Discussion

In this section, we compare our work with other state-of-the-art localization systems. Since it is hard to setup exactly same experimental deployment, it is hard for us to directly compare the experimental performance of our approach with other existing similar solutions. Nevertheless, we have performed some high level comparison analysis and the findings are summarized in Table 4.

From the table, it is clear that our proposed localization system has several advantages, including very low hardware cost, less pre-calibration burden (low training overhead), easy extension to larger areas (high potential in scalability), maintenance free, and high accuracy compared with other device-free passive localization systems.

7. CONCLUSION

RFID-based localization and tracking has some promising potentials. In this paper, we present the design, implementation, and evaluation of a device-free RFID-based localization method based on probabilistic classification, using pure passive RFID tags. We explore three learning-based classification methods to deal with localization problem. We propose to model RSSI distribution at each grid as a multivariate Gaussian Mixture Model, and Expectation Maximization is used to learn the maximum likelihood estimates of the model parameters. This approach enables us to localize the subject based on the maximum a posteriori estimation. We further introduce multivariate Gaussian mixture models based HMM and k NN based HMM to track a moving subject based on continuous sequence of RSSI. We validate and evaluate our proposed approaches using a testbed consisting of pure passive RFID tags. The results demonstrate the feasibility and effectiveness of our approaches.

The experimental results show that the performance of our approach in tracking a moving subject is relatively worse than localizing a stationary subject. In our future work, we will investigate how to improve the accuracy in real-time tracking by reducing RSSI noise and extracting more informative and distinctive features. We will also study how to enhance our approach to enable multi-subjects localization and tracking.

Table 4: Comparison of different device-free passive localization systems

Items	Active Tags [4, 20]	RTI [21]	NUZZER [11]	SCPL [15]	Ichnaea [9]	TagTrack
Measured Physical Quantity	RSS threshold	RSS attenuation	RSS changes	RSS changes	RSS changes	RSS variance
Hardware Cost	High	High	Medium	Medium	Medium	Low
Non-LoS Localization	No	No	Yes	Yes	Yes	Yes
Complexity of Single Node/device	Medium	Medium	Medium	Medium	Medium	Low
Training Overhead	Low	Low	High	Medium	Low	Low
Potential Scalability	Medium	Low	High	Medium	High	High
Accuracy	Medium	High	High	Medium	Medium	High
Maintenance (Replace battery etc.)	Medium	High	Medium	Medium	Medium	Low

8. REFERENCES

- [1] H. Akaike. A new look at the statistical model identification. *IEEE Transactions on Automatic Control*, 19(6):716–723, Dec 1974.
- [2] C.-C. Chang and C.-J. Lin. LIBSVM: A library for support vector machines. *ACM Transactions on Intelligent Systems and Technology*, 2(3):27:1–27:27, 2011.
- [3] J. Han, C. Qian, X. Wang, D. Ma, J. Zhao, P. Zhang, W. Xi, and Z. Jiang. Twins: Device-free object tracking using passive tags. In *Proceedings of the 33rd IEEE International Conference on Computer Communications (INFOCOM)*, pages 469–476, 2014.
- [4] Y. Liu, L. Chen, J. Pei, Q. Chen, and Y. Zhao. Mining frequent trajectory patterns for activity monitoring using radio frequency tag arrays. In *Proceedings of 5th IEEE International Conference on Pervasive Computing and Communications (PerCom)*, pages 37–46, 2007.
- [5] L. M. Ni, Y. Liu, Y. C. Lau, and A. P. Patil. Landmarc: indoor location sensing using active rfid. *Wireless networks*, 10(6):701–710, 2004.
- [6] L. M. Ni, D. Zhang, and M. R. Souryal. Rfid-based localization and tracking technologies. *IEEE Wireless Communications*, 18(2):45–51, 2011.
- [7] N. B. Priyantha, A. Chakraborty, and H. Balakrishnan. The cricket location-support system. In *Proceedings of the 6th Conference on Mobile Computing and Networking (MobiCom)*, pages 32–43, 2000.
- [8] C. Qian, H. Ngan, Y. Liu, and L. M. Ni. Cardinality estimation for large-scale rfid systems. *IEEE Transactions on Parallel and Distributed Systems*, 22(9):1441–1454, 2011.
- [9] A. Saeed, A. Kosba, and M. Youssef. Ichnaea: A low-overhead robust wlan device-free passive localization system. *IEEE Journal of Selected Topics in Signal Processing*, 8(1):5–15, 2014.
- [10] M. Seifeldin and M. Youssef. A deterministic large-scale device-free passive localization system for wireless environments. In *Proceedings of the 3rd Intl. Conf. on Pervasive Technologies Related to Assistive Environments*, page 51, 2010.
- [11] M. Seifeldin et al. Nuzzer: A Large-Scale Device-Free Passive Localization System for Wireless Environments. *Mobile Computing, IEEE Transactions on*, 12(7):1321–1334, July 2013.
- [12] B. Wagner, N. Patwari, and D. Timmermann. Passive rfid tomographic imaging for device-free user localization. In *The 9th Workshop on Positioning Navigation and Communication (WPNC)*, pages 120–125, 2012.
- [13] P. Wilson, D. Prashanth, and H. Aghajan. Utilizing rfid signaling scheme for localization of stationary objects and speed estimation of mobile objects. In *2007 IEEE International Conference on RFID*, pages 94–99, 2007.
- [14] C. Wu, Z. Yang, Y. Liu, and W. Xi. Will: Wireless indoor localization without site survey. *IEEE Transactions on Parallel and Distributed Systems*, 24(4):839–848, 2013.
- [15] C. Xu, B. Firner, R. S. Moore, Y. Zhang, W. Trappe, R. Howard, F. Zhang, and N. An. SCPL: Indoor Device-free Multi-subject Counting and Localization Using Radio Signal Strength. In *Proceedings of the 12th International Conference on Information Processing in Sensor Networks (IPSN)*, pages 79–90, 2013.
- [16] C. Xu, B. Firner, Y. Zhang, R. Howard, J. Li, and X. Lin. Improving rf-based device-free passive localization in cluttered indoor environments through probabilistic classification methods. In *Proceedings of the 11th Intl. Conf. on Information Processing in Sensor Networks (IPSN)*, pages 209–220, 2012.
- [17] L. Yao, W. Ruan, Q. Z. Sheng, X. Li, and N. J. Falkner. Exploring tag-free rfid-based passive localization and tracking via learning-based probabilistic approaches. In *Proc. of the 23rd ACM Intl. Conference on Information and Knowledge Management (CIKM)*, Shanghai, China, 2014.
- [18] H. Ye, T. Gu, X. Zhu, J. Xu, X. Tao, J. Lu, and N. Jin. Ftrack: Infrastructure-free floor localization via mobile phone sensing. In *Proceedings of the 10th IEEE International Conference on Pervasive Computing and Communications (PerCom)*, pages 2–10, 2012.
- [19] M. Youssef, M. Mah, and A. Agrawala. Challenges: Device-free passive localization for wireless environments. In *Proceedings of the 13th Annual ACM International Conference on Mobile Computing and Networking (MobiCom)*, pages 222–229, 2007.
- [20] D. Zhang, J. Zhou, M. Guo, J. Cao, and T. Li. Tasa: Tag-free activity sensing using rfid tag arrays. *IEEE Transactions on Parallel and Distributed Systems*, 22(4):558–570, 2011.
- [21] Y. Zhao, N. Patwari, J. M. Phillips, and S. Venkatasubramanian. Radio tomographic imaging and tracking of stationary and moving people via kernel distance. In *Proceedings of the 12th International Conference on Information Processing in Sensor Networks (IPSN)*, pages 229–240, 2013.